J Mater Sci (2008) 43:4220–4225
DOI 10.1007/s10853-008-2610-5

Dielectric properties of $Pb[(1-x)(Zr_{1/2}Ti_{1/2})-x(Zn_{1/3}Ta_{2/3})]O_3$ ceramics prepared by columbite and wolframite methods

Wanwimon Banlue · Naratip Vittayakorn · Chien-Chih Huang · David P. Cann

Received: 15 January 2008 / Accepted: 24 March 2008 / Published online: 9 April 2008

Abstract Polycrystalline samples of $Pb[(1-x)(Zr_{1/2}Ti_{1/2})-x(Zn_{1/3}Ta_{2/3})]O_3$, where $x = 0.1$–0.5 were prepared by the columbite and wolframite methods. The crystal structure, microstructure, and dielectric properties of the sintered ceramics were investigated as a function of composition via X-ray diffraction (XRD), scanning electron microscopy (SEM), and dielectric spectroscopy. The results indicated that the presence of $Pb(Zn_{1/3}Ta_{2/3})O_3$ (PZnTa) in the solid solution decreased the structural stability of overall perovskite phase. A transition from tetragonal to pseudo-cubic symmetry was observed as the PZnTa content increased and a co-existence of tetragonal and pseudo-cubic phases was observed at a composition close to $x = 0.1$. Examination of the dielectric spectra indicated that PZT–PZnTa exhibited an extremely high relative permittivity at the MPB composition. The permittivity showed a ferroelectric to paraelectric phase transition at 330 °C with a maximum value of 19,600 at 100 Hz at the MPB composition.

Introduction

Lead zirconate titanate $Pb(Zr_{1-x}Ti_x)O_3$ perovskite solid solutions (PZT) are normal ferroelectric ceramic materials with many important practical applications including piezoelectric devices, ferroelectric memories, high ε capacitors, and infrared pyroelectric detectors, by utilizing their excellent piezoelectric, ferroelectric, and pyroelectric properties [1, 2]. The anomalous piezoelectric properties of PZT ceramics near the morphotropic phase boundary (MPB) separating two ferroelectric phases, namely, rhombohedral and tetragonal phases at low and high Ti contents, respectively [3]. Recently, the new free energy formulation automatically predicts equilibrium PZT phase diagram with two-phase region replacing the linear MPB and satisfying the Gibbs phase rule [4]. Identifying the MPB in the phase equilibria in ferroelectric systems is very important in order to obtain the optimum electrical properties. Therefore, most commercial ferroelectric ceramics are designed in the vicinity of the MPB with various doping schemes in order to take advantage of the superior dielectric and piezoelectric properties [5, 6].

Recently, many piezoelectric ceramic materials have been developed from binary systems containing a combination of normal ferroelectrics with tetragonal symmetry and relaxor ferroelectrics with rhombohedral symmetry near the MPB. These systems can yield high dielectric permittivities such as in PMN–PT [7] and PZN–PT [8], excellent piezoelectric coefficients such as in PZN–PZT [9] and PSN–PT [10], and high pyroeletric coefficients such as in PNN–PT–PZ [11]. The low phase-transition temperature of some members of the lead-based tantalate family $Pb(B_{1-x}Ta_x)O_3$, in which B is Zn^{2+}, Mg^{2+} and Ni^{2+}, make them important candidates for utilization in devices such as low-temperature capacitors and actuators for space applications [12]. Lead zinc tantalate $Pb(Zn_{1/3}Ta_{2/3})O_3$ solid solutions (PZnTa) possess the perovskite structure and exhibit relaxor ferroelectric behavior. Nevertheless, synthesis of perovskite lead zinc tantalate $Pb(Zn_{1/3}Ta_{2/3})O_3$

W. Banlue · N. Vittayakorn (✉)
Materials Science Research Unit, Department of Chemistry, Faculty of Science, King Mongkut's Institute of Technology Ladkrabang, Bangkok 10520, Thailand
e-mail: naratipcmu@yahoo.com

C.-C. Huang · D. P. Cann
Materials Science, School of Mechanical, Industrial, and Manufacturing Engineering, Oregon State University, Corvallis, OR 97331, USA

(PZnTa) has been unsuccessful until now [13]. It is well-known that during the phase-formation process of lead-based perovskite materials a pyrochlore-type phase ($A_2B_2O_{7-\delta}$) with low dielectric permittivity precedes the formation of the perovskite phase. The failure can be attributed to the higher covalency of Zn^{2+} and Ta^{5+} as well as to the somewhat larger ionic size of Zn^{2+} as compared to the sixfold lattice sites formed by the oxygen octrahedra. A columbite–wolframite process was then introduced to promote the development of the perovskite phase and to suppress the formation of the pyrochlore phase [13–15].

Since both PZT and PZnTa have the perovskite structure, it is suggested that PZnTa can be alloyed with PZT in order to stabilize and optimize the PZnTa ceramics. Recently our previous work [9, 16] has shown promise in producing phase-pure perovskite solid solutions based on $Pb(Zr_{1/2}Ti_{1/2})O_3$–$Pb(Zn_{1/3}Nb_{2/3})O_3$ (PZT–PZN) via the columbite method. The binary system of $(1-x)$PZT $-$ xPZN exhibited two MPBs at the compositions $x = 0.5$ and $x \sim 0.2$–0.3. The maximum value of d_{33} (>600 pC/N) and the highest k_p ($\sim$0.7) were recorded for the composition $x = 0.3$. In addition, Nb and Ta belong to the same group in the periodic table and the have the same ionic radii. It is expected that excellent properties can be obtained from ceramics in PZT–PZnTa system. So far, there have been no systematic studies on the structural and dielectric properties over the entire range of PZT–PZnTa solid solutions. In the present study, PZT and PZnTa were chosen as end components to prepare solid solutions via a columbite–wolframite precursor method. Crystal structure and microstructure were investigated by XRD and SEM analysis, respectively. Finally, the dielectric properties of PZT–PZnTa ceramics were determined as a function of temperature and frequency to establish structure–property relationships.

Experimental

The perovskite-phase powders were synthesized using a columbite–wolframite precursor method in order to avoid the formation of a pyrochlore phase. Powders of ZnO (99.9%), Ta_2O_5 (99.9%), PbO (Fluka, >99% purity), TiO_2 (99.8%), and ZrO_2 (99%) were used as the starting materials. The following reaction sequences are proposed for the formation of PZT–PZnTa:

$$ZnO_{(s)} + Ta_2O_{5(s)} \rightarrow ZnTa_2O_{6(s)} \quad (1)$$

$$ZrO_{2(s)} + TiO_{2(s)} \rightarrow ZrTiO_{4(s)} \quad (2)$$

$$PbO_{(s)} + (1-x)/2\ ZrTiO_{4(s)} + x/3\ ZnTa_2O_{6(s)} \rightarrow Pb\left[(1-x)\left(Zr_{1/2}Ti_{1/2}\right) - x\left(Zn_{1/3}Ta_{2/3}\right)\right]O_{3(s)} \quad (3)$$

The columbite precursor $ZnTa_2O_6$ was prepared from the reaction between ZnO and Ta_2O_5 at 1,100 °C for 4 h and then ZrO_2 was reacted with TiO_2 at 1,400 °C for 4 h to form $ZrTiO_4$. The precursors $ZnTa_2O_6$, $ZrTiO_4$ and PbO (with 2 mol% excess PbO) were weighed according to the compositions of $Pb[(1-x)(Zr_{1/2}Ti_{1/2}) - x(Zn_{1/3}Ta_{2/3})]O_3$ with $x = 0.1$–0.5. Each mixture of the starting powders was milled and mixed in a ball mill, as well as wet-homogenized with ethanol using nylon-coated YTZ zirconia milling as media for 18 h. After drying, the mixtures were calcined at 700–950 °C for 4 h in an alumina crucible and configured with a heating rate of 20 °C/min. The calcined powders were milled for 3 h in order to reduce the particle size. After grinding and sieving, the calcined powders were mixed with 5 wt% polyvinyl alcohol binder and uniaxially pressed into pellets. Binder burnout occurred by slowly heating to 500 °C and holding for 2 h. Sintering occurred between 1,100 and 1,250 °C with a dwell time of 4 h. To mitigate the effects of lead loss during sintering, the pellets were sintered in a closed alumina crucible containing $PbZrO_3$ powder. PZT–PZnTa ceramics were subsequently examined by room temperature X-ray diffraction (XRD; Philips PW 1729 diffractometer), using Ni-filtered CuK_α radiation to identify the perovskite structure. The relative amounts of perovskite and pyrochlore phase were then determined by measuring the primary X-ray peak intensities of the perovskite and pyrochlore phase. The density of the sintered PZT–PZnTa pellets was measured by the water immersion method (Archimedes method). The relative density of all the sintered pellets in this study was approximately 94–96% of the theoretical density. To determine the dielectric properties, the maximum density sample for each composition samples was ground on both surfaces and silver electrodes were applied using a low-temperature silver paste by firing at 500 °C for 30 min. The capacitance was measured with a HP4284A LCR meter in connection with a sample holder (Norwegian Electroceramics) capable of high temperature measurement. The relative permittivity (ε_r) was calculated using the geometric area and thickness of the discs.

Result and discussion

The XRD patterns of $(1-x)$PZT $-$ xPZnTa ceramics with various x values are shown in Fig. 1. The patterns show a single-phase perovskite for the compositions $x = 0.1$ and 0.2. A cubic pyrochlore phase $Pb_{1.83}(Zn_{0.29}Ta_{1.71})O_{6.39}$ (Powder diffraction Files No. 34-395), identified with "*", began to develop at $x = 0.3$ and increased in intensity with increasing PZnTa concentration. No evidence of a cubic phase of $Pb_{1.49}Ta_2O_{6.28}$ (Powder diffraction Files No. 84-1732) was found. These results indicate that the presence of PZnTa in the solid solution decreased the structural stability of the PZT perovskite phase due to its tolerance factor and electronegativity [13]. It is interesting to note that the pure

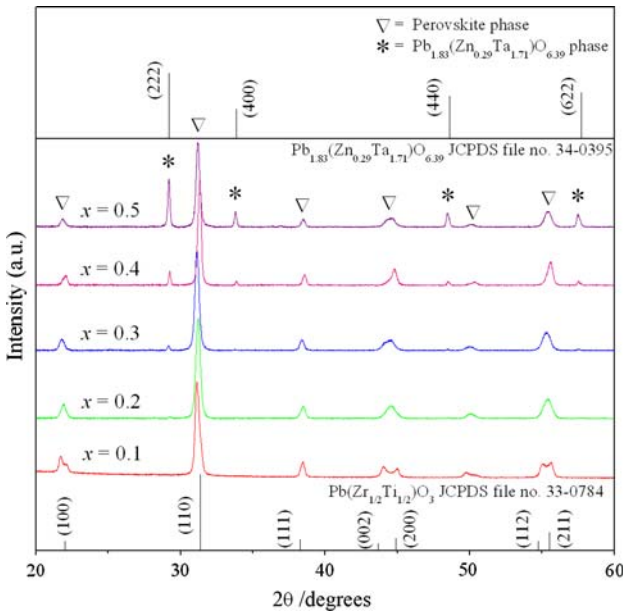

Fig. 1 XRD patterns of $(1 - x)$PZT $- x$PZnTa ceramics prepared by columbite–wolframite method as a function of composition

perovskite phase in $(1 - x)$PZT $- x$PZnTa can only be obtained for $x \leq 0.2$. This is a significant contrast to the $(1 - x)$PZT $- x$Pb$(Zn_{1/3}Nb_{2/3})O_3$ system in which the perovskite phase can be obtained up to $x \leq 0.5$. The results indicate that it is more difficult to obtain a pure perovskite phase in tantalate systems than in niobates.

Although Nb and Ta belong to the same periodic group, Ta^{5+} has stronger covalent properties [17]. It is well known that an increase in covalent bond strength decreases the thermodynamic stability of the perovskite structure [13]. This is likely the main reason it is difficult to obtain the perovskite phase in the tantalate system. Studies on the stabilization of the perovskite phase in solid solutions of PZN and PZnTa with BT, PMN and PMT also showed an easier stabilization of the perovskite structure in PZN, due to the higher ionic strength of Nb–O bonds [18].

SEM micrographs of a fractured surface of PZT–PZnTa ceramics are shown in Fig. 2a and b, respectively. The micrograph of 0.9PZT–0.1PZnTa (Fig. 2a) shows a highly homogeneous microstructure. These micrographs indicate that average grain size was in the range of 1.27 μm, and the fracture occurred mostly by intergranular mechanisms. The 0.5PZT–0.5PZnTa ceramic showed a very heterogeneous microstructure (Fig. 2b) with a large amount of pyrochlore phase, as XRD patterns also indicated.

The $PbZrO_3$–$PbTiO_3$ phase diagram predicts that at room temperature $Pb(Zr_{1/2}Ti_{1/2})O_3$ falls within the tetragonal phase field near the MPB. The crystal symmetry for PZnTa-based perovskite is cubic at room temperature. Below the phase transition temperature the symmetry changes to rhombohedral. Since PZnTa has a low phase

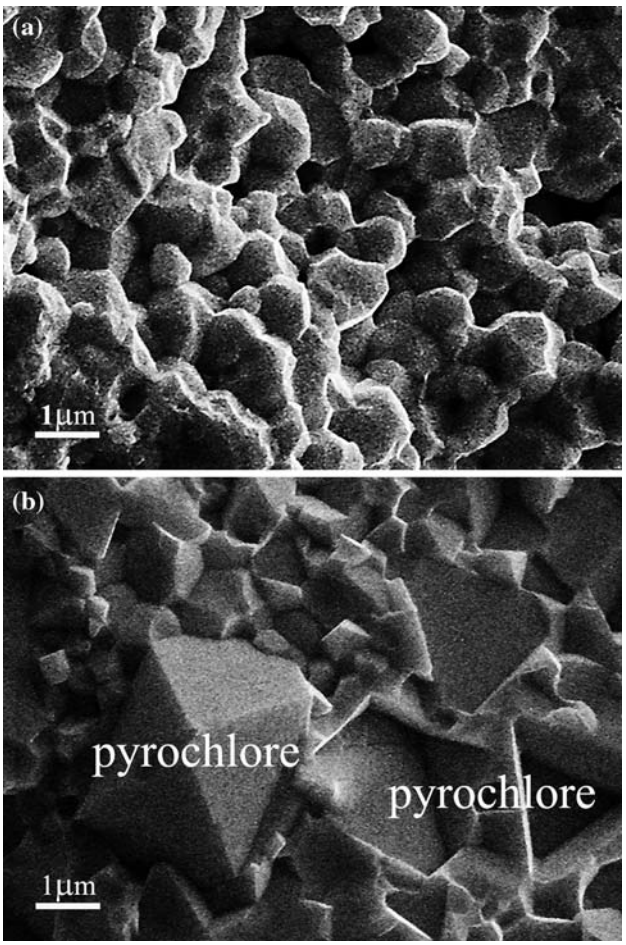

Fig. 2 SEM images of the grain morphology in $(1 - x)$PZT $- x$PZnTa ceramics for (**a**) $x = 0.1$ and (**b**) $x = 0.5$

transition temperature, with increasing x the crystal symmetry should change due to the decrease in phase transition temperature. It is well known that in the pseudo-cubic phase the {2 0 0} profile will show a single narrow peak because all the planes of {2 0 0} share the same lattice parameters, while in the tetragonal phase the {2 0 0} profile should be split into two peaks with the intensity height of the former being half of the latter because the lattice parameters of (2 0 0) and (0 2 0) are the same but are slightly different from those of (0 0 2).

Figure 3 shows the evolution of the (2 0 0) peak as a function of composition. At low PZnTa concentrations, the XRD pattern shows strong (200) peak splitting which is indicative of tetragonal symmetry. As the PZnTa concentration increased, the (2 0 0) reflection transformed to a single peak which suggests pseudo-cubic symmetry. To a first approximation, it could be said that the composition with $x = 0.1$ is close to the MPB, where the structure of the PZT–PZnTa compositions gradually shifts from tetragonal to pseudo-cubic symmetry as the PZnTa content increased. Dielectric data described later further supports this

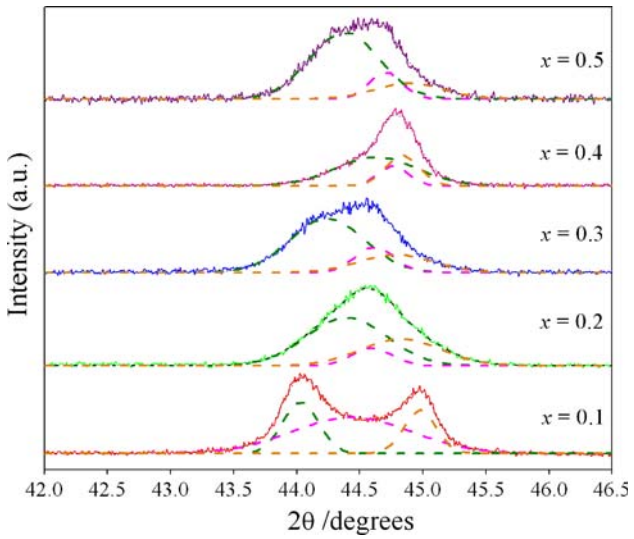

Fig. 3 XRD pattern of the (200) peak of $(1 - x)$PZT $- x$PZnTa ceramics, for $x = 0.0$–0.5

assumption. It is interesting to note that the influence of the addition of PZnTa on the phase transition of $Pb(Zr_{1/2}Ti_{1/2})O_3$ is similar to that of the $Pb(Zr_{1/2}Ti_{1/2})O_3$–$Pb(Ni_{1/3}Nb_{2/3})O_3$, $Pb(Zr_{1/2}Ti_{1/2})O_3$–$Pb(Co_{1/3}Nb_{2/3})O_3$, and $Pb(Zr_{1/2}Ti_{1/2})O_3$–$Pb(Zn_{1/3}Nb_{2/3})O_3$ systems [9, 19–21].

The characteristic temperature dependence of the dielectric constant at 100 Hz for $(1 - x)$PZT $- x$PZnTa, where $x = 0.1$–0.5, is shown in Fig. 4. The transition temperatures and maximum dielectric constants of the 0.9PZT–0.1PZnTa ceramics in this work were 330 °C and 19,600, respectively. The frequency dependence of dielectric properties for $x = 0.1$ and 0.5 ceramics are shown in Fig. 5a and b. For 0.9PZT–0.1PZnTa (Fig. 5a), the dielectric constants peak is sharp and approaches19,600. The dielectric properties of 0.9PZT–0.1PZnTa ceramic change significantly with

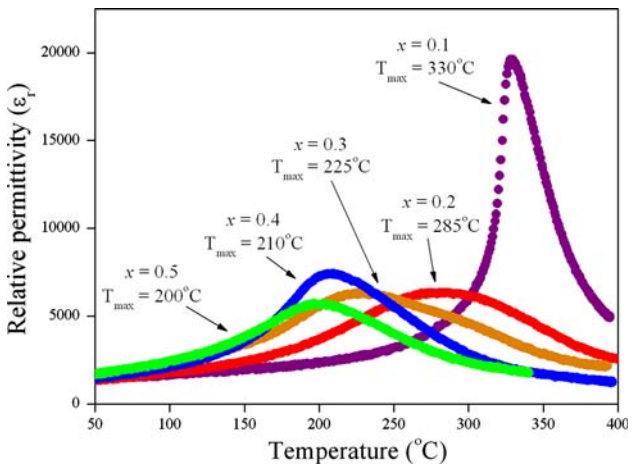

Fig. 4 Variation of the dielectric constant with temperature for $(1 - x)$ PZT $- x$PZnTa ceramics at 100 Hz

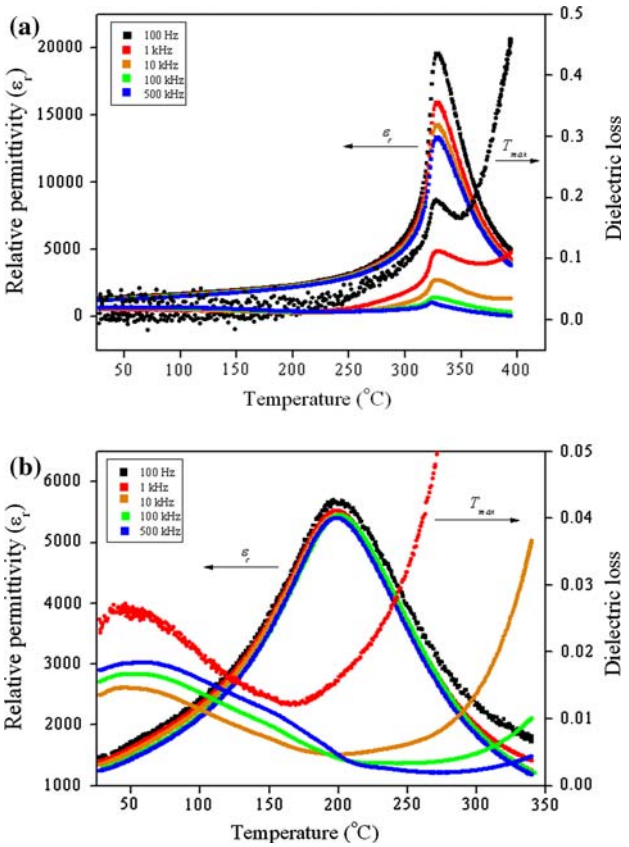

Fig. 5 Temperature and frequency dependence of the dielectric properties for: (**a**) $x = 0.1$ and (**b**) $x = 0.5$ ceramics

temperature, but are nearly independent of frequency, except in the vicinity of the phase transformation temperature [22, 23]. This is a typical characteristic of ferroelectric ceramics with a long-range ordered structure. It is well known that PZT exhibits normal ferroelectric behavior and PZnTa is a relaxor ferroelectric material as a result of a short-range ordered structure with a nanometer scale compositional heterogeneity [24]. The nature of the homogeneously polarized states is believed to be primarily controlled by the concentration of PZnTa. When PZnTa is added to form the binary system with PZT, a clear shift of the transition temperature to lower temperatures was observed. Furthermore, the dielectric peak broadened indicating an increase in the diffuseness of the phase transition. It should also be noted here that, in all compositions, the dielectric properties increased significantly at high temperatures as a result of thermally activated space charge conduction. The variation in the transition temperature with composition and other dielectric data is listed in Table 1. The Curie temperature significantly decreased with increasing PZnTa content up to 30 mol%. However, for the compositions $0.3 \leq x \leq 0.5$, transition temperature remained at a nearly constant value between 200 and 225 °C. This is consistent with the X-ray

diffration findings that indicated the co-existence of a pyrochlore phase for these compositions.

A modified Curie–Weiss law can be used to model the dielectric behavior of a normal ferroelectric in solid solution with a relaxor ferroelectric with a diffuse phase transition. The formulation is as follows:

$$\frac{\varepsilon'_{\mathrm{m}}}{\varepsilon'(f,\ T)} = 1 + \frac{(T - T_{\mathrm{m}}(f))^{\gamma}}{2\delta_{\gamma}^{2}} \tag{4}$$

where $1 \leq \gamma \leq 2$. When $\gamma = 1$, Eq. 4 simplifies to the Curie–Weiss law; when $\gamma = 2$ this equation describes the ideal relaxor behavior with a quadratic dependence. The

Table 1 Dielectric properties of $(1 - x)$PZT $- x$PZnTa ceramics at 100 Hz

PZTa content (x)	ε_r at room temp.	tan δ at room temp.	$T_{\max}$ (°C)	ε_r at $T_{\max}$	tan δ at $T_{\max}$	δ_γ (°C)	γ
0.1	1,430	0.0102	330	19,600	0.193	13.51	1.74
0.2	1,280	0.0429	285	6,310	0.081	22.36	1.98
0.3	1,500	0.0282	225	6,290	0.066	21.11	1.89
0.4	1,340	0.0289	210	7,410	0.072	12.57	1.80
0.5	1,520	0.0163	200	5,690	0.039	11.87	1.72

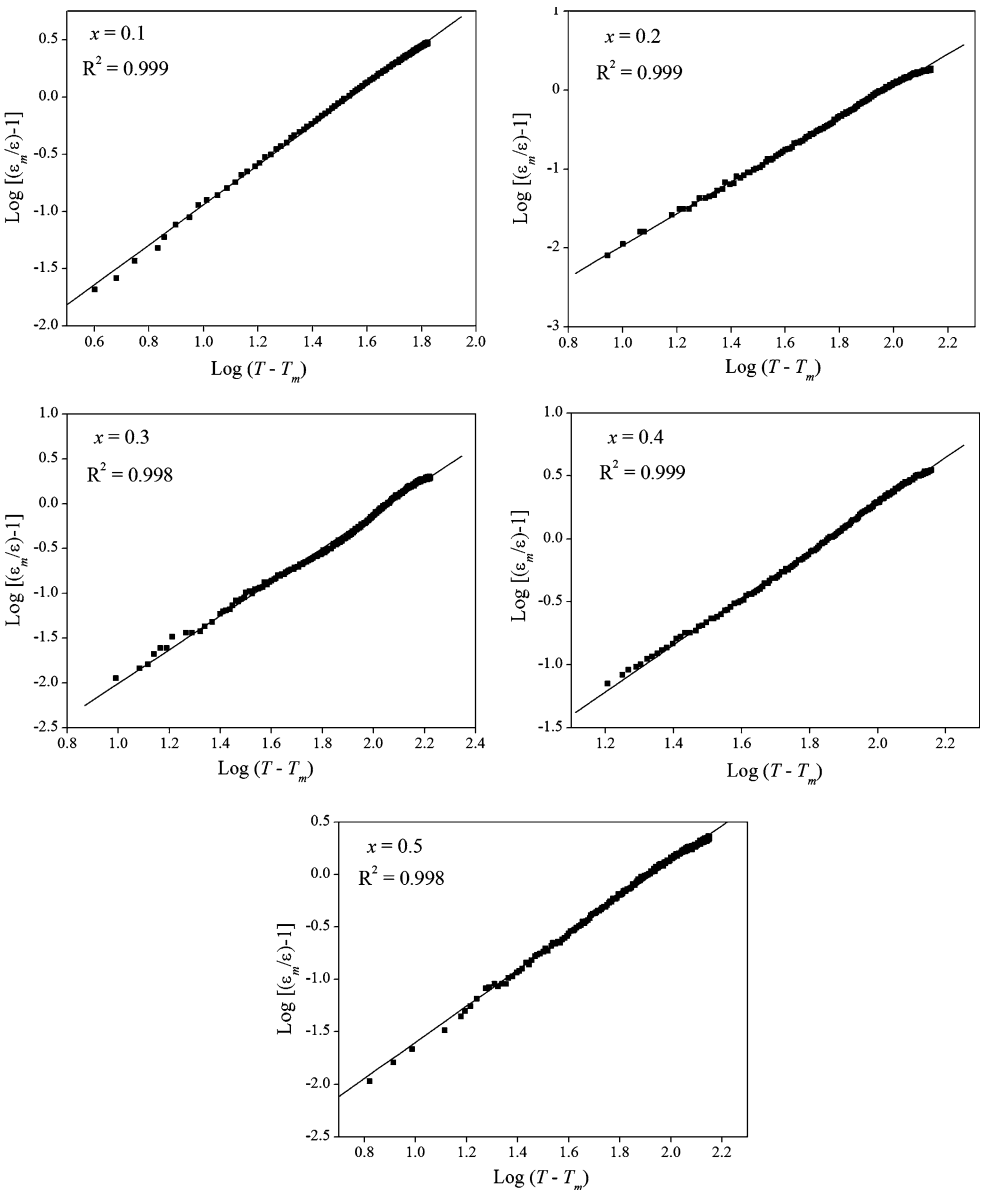

Fig. 6 Plots of $\log[(\varepsilon_{\mathrm{m}}/\varepsilon) - 1)]$ vs. $\log(T - T_{\mathrm{m}})$ for $(1 - x)$ PZT $- x$PZnTa ceramics. The solid lines are fits to Eq. 5. γ, δ and R^2 indicate fitting parameters (γ and δ) and correlation of the fit (R^2)

parameter ε'_m is the maximum value of the relative permittivity at $T = T_m$ (f) and $\varepsilon'(f, T)$ is the relative permittivity of the sample. If $\log[\varepsilon'_m/\varepsilon'(f, T) - 1]$ is plotted versus $\log[T - T_m(f)]$, the values of γ and δ_γ can be determined as seen in Fig. 6. The parameter γ was determined to be in the range of 1.72–1.98 and the diffuseness parameter δ_γ was measured to be 11.87–22.36, which confirms the diffuse phase transitions in PZT–PZnTa due to a high degree of disorder. The calculations suggest that the addition of PZnTa into PZT leads to lower degree of disorder but can be attributed to the pyrochlore phase present in high PZnTa-content compositions.

Conclusions

Ceramic solid solutions based on $(1 - x)$ $Pb(Zr_{1/2}Ti_{1/2})O_3 - (x)Pb(Zn_{1/3}Ta_{2/3})O_3$ (where $x = 0.1$, 0.2, 0.3, 0.4, and 0.5) were prepared via a columbite–wolframite method. The PZT–PZnTa solid solutions exhibit a single-phase perovskite structure for $x \leq 0.2$. As the content of PZnTa increases (i.e., $x \geq 0.3$), a secondary pyrochlore phase $Pb_{1.83}(Zn_{0.29}Ta_{1.71})O_{6.39}$ was formed. The results indicate that it is more difficult to obtain pure perovskite in tantalate solid solutions than it is in niobates solid solutions. The dielectric response of 0.9PZT–0.1PZnTa is closer to normal ferroelectric behavior, while the other compositions exhibit a diffuse phase transition. Investigations of the structure and properties of the PZT–PZnTa system over the range $x = 0.1$–0.5 have revealed an MPB at $x = 0.1$, separating a tetragonal phase from a pseudocubic phase. Examination of the dielectric spectra indicates that PZT–PZnTa exhibits a high relative permittivity at the MPB composition. The permittivity shows a ferroelectric to paraelectric phase transition at 330 °C with a maximum value of 19,600 at 100 Hz at the MPB composition.

Acknowledgements This work was supported by the Thailand Research Fund (TRF), the Commission on Higher Education (CHE), the National Research Council of Thailand (NRCT), and the King Mongkut's Institute of Technology Ladkrabang (KMITL).

References

1. Uchino K (2000) Ferroelectric devices. Marcel Dekker, Inc., New York
2. Bhalla AS, Guo R, Roy R (2000) Mat Res Innovat 4:3. doi: 10.1007/s100190000062
3. Jaffe B, Cook WR (1971) Piezoelectric ceramic. R.A.N. Publishers
4. George A Rossetti J, Zhang W, Khachaturyan AG (2006) Appl Phys Lett 88:072912. doi:10.1063/1.2173721
5. Haertling GH (1999) J Am Ceram Soc 82:797
6. Xu Y (1991) Ferroelectric materials and their application. Elsevier Science Publishers B.V
7. Seung-Eek P, Shrout TR (1997) IEEE Trans Ultrason Ferroelectr Freq Control 44:1140
8. Takenaka T, Muramata K, Fujii T (1992) Ferroelectrics 134:133. doi:10.1080/00150199208015577
9. Vittayakorn N, Puchmark C, Rujijanagul G, Tan X, Cann DP (2006) Curr Appl Phys 6:303
10. Bing Y-H, Ye Z-G (2006) J Cryst Growth 287:326. The 16th American Conference on Crystal Growth and Epitaxy – ACCGE 16
11. Cornejo IA, Jadidian B, Akdogan EK, Safari A (1998) Dielectric and Electromechanical properties of PNN–PT–PZ system: a processing-property study. In: Proc IEEE ISAF'98
12. Kuwata J, Uchino K, Nomura S (1982) Jpn J Appl Phys 21:1298
13. Shrout TR, Halliyal A (1987) Am Ceram Soc Bull 66:704
14. Vittayakorn N, Wirunchit S (2007) Smart Mater Struct 16:851
15. Vittayakorn N, Rujijanagul G, Tunkasiri T, Tan X, Cann DP (2003) J Mater Res 18:2882
16. Vittayakorn N, Rujijanagul G, Tunkasiri T, Tan X, Cann DP (2004) Mater Sci Eng B 108:258
17. Ahn B-Y, Kim N-K (2002) J Mater Sci 37:4697
18. Kim J-S, Kim N-K (2003) J Am Ceram Soc 86:929
19. Vittayakorn N, Rujijanagul G, Tan X, He H, Marquardt MA, Cann DP (2006) J Electroceram 16:141
20. Vittayakorn N, Rujijanagul G, Tan X, Marquardt MA, Cann DP (2004) J Appl Phys 96:5103
21. Vittayakorn N, Tunkasiri T (2007) Phys Scr T129:199
22. Koval V, Alemany C, Brianin J, Bruncková H (2004) J Electroceram 10:19
23. Yimnirun R, Ananta S, Laoratanakul P (2005) J Eur Ceram Soc 25:3235
24. Randall CA, Bhalla AS, Shrout TR, Cross LE (1990) Ferroelectrics 11:103